**RESEARCH ARTICLE** OPEN ACCESS

# High-Dimensional Immunophenotyping of Post-COVID-19 and Post-Influenza Patients Reveals Persistent and Specific Immune Signatures After Acute Respiratory Infection

Francisco Pérez-Cózar[1] | Paloma Cal-Sabater[2] | Paulina Rybakowska[1] | Elisa Arribas-Rodríguez[2] | Aida Fiz-López[2] | Antonio García-Blesa[2] | Juan Hernández[2] | Sara Gutiérrez[3] | Pablo Tellería[3] | Cristina Novoa[3] | Silvia Rojo Rello[4] | Ángel De Prado[2] | Cándido Pérez[2] | Rosa Sedano[3] | Marta Domínguez-Gil[5] | María Jesús Peñarrubia[6] | Daan K. J. Pieren[7] | José A. Garrote[2] | Eduardo Arranz[2] | José María Eiros[4] | Eduardo Tamayo[8] | Antonio Orduña[5] | Cécile A.C.M. van Els[7] | Carlos Dueñas[3] | Concepción Marañón[1] | David Bernardo[9] | Sara Cuesta-Sancho[9] 🆔

[1]Pfizer-University of Granada-Junta de Andalucía Centre for Genomics and Oncological Research (GENYO). Pfizer/University of Granada/Andalusian Regional Government, PTS Granada, Granada, Spain | [2]Mucosal Immunology Lab. Institute of Biomedicine and Molecular Genetics (IBGM, University of Valladolid-CSIC), Valladolid, Spain | [3]Internal Medicine Department, Hospital Clínico Universitario de Valladolid, Valladolid, Spain | [4]Microbiology Unit, Hospital Clínico Universitario de Valladolid, Valladolid, Spain | [5]Microbiology Department, Hospital Universitario Rio Hortega, Valladolid, Spain | [6]Department of Hematology, Hospital Clínico Universitario de Valladolid, Valladolid, Spain | [7]Centre for Infectious Disease Control, National Institute for Public Health and the Environment, Bilthoven, The Netherlands | [8]Department of Surgery, Faculty of Medicine, Centro de Investigación Biomédica en Red de Enfermedades Infecciosas (CIBERINFEC), Instituto de Salud Carlos III, Madrid, Universidad de Valladolid, Valladolid, Spain | [9]Mucosal Immunology Lab, Department of Paediatrics and Immunology, University of Valladolid, Valladolid, Spain

**Correspondence:** Concepción Marañón (concepcion.maranon@genyo.es) | David Bernardo (d.bernardo.ordiz@gmail.com) | Sara Cuesta-Sancho (sara.cuesta.uva@gmail.com)

## ABSTRACT

Long-term consequences of SARS-CoV-2 infection are unknown since recovered individuals can experience symptoms and latent viral reactivation for months. Indeed, acute post-infection sequelae have also been observed in other respiratory viral infections, including influenza. To characterize post-COVID-19 and post-influenza induced alterations to the cellular immunome, peripheral blood mononuclear cells (PBMCs) were obtained from patients 3 months after recovery from COVID-19 ($n = 93$) or influenza ($n = 25$), and from pre-pandemic healthy controls ($n = 25$). PBMCs were characterized using a 40-plex mass cytometry panel. Principal component analysis (PCA), classification models, and K-means clustering were subsequently applied. PCA identified distinct immune profiles between cohorts, with both post-COVID and post-flu patients displaying an altered chemokine receptor expression compared to pre-pandemic healthy controls. These alterations were more prominent in post-COVID patients since they exhibited highly increased expression of chemokine receptors CXCR3 and CCR6 by various lymphoid populations, while post-influenza patients mainly showed a decrease in CCR4 expression by naïve T cells, monocytes, and conventional dendritic cells. Classification models using immunophenotyping data confirm the three groups, while

---

K-means clustering revealed two subgroups among post-COVID patients, with younger patients showing more pronounced immune alterations in the chemokine receptor profile, independently of long COVID symptoms. In conclusion, post-COVID and post-influenza patients exhibit distinct and unique persistent immune alterations. Understanding these altered immune profiles can guide targeted therapies for post-COVID syndrome and highlight differences in immune recovery from various respiratory infections.

## 1 | Introduction

In the last 4 years, the acute phase of COVID-19 has been extensively studied and described [1]. Briefly, the initial viral load and the efficacy of the innate immune response, particularly mediated by Type I interferons, appear to be critical for both the subsequent adaptive response and the clinical outcome [2]. Many patients with acute SARS-CoV-2 infection have profound lymphocytopenia, which is associated with a poor clinical outcome [3]. Accordingly, peripheral lymphopenia and altered frequencies of innate and adaptative cell subsets such as $CD4^+$ and $CD8^+$ T cells, as well as NK cells, were associated with acute SARS-CoV-2 infection [4].

Independent of the severity of the acute COVID-19 or flu infection, recovered individuals can present virus reactivation mainly by EBV, HHV-1, and CMV [5, 6]. Post-viral syndrome is a complex condition characterized by persistent pain, fatigue, and neurocognitive difficulties, and can last for weeks, months, or even years after acute infection with SARS-CoV-2, influenza, or Dengue, among others, hence constituting a significant challenge for public health [7, 8]. Long COVID (LC) is therefore defined by the World Health Organization (WHO) as the continuation or development of new symptoms 3 months after the initial SARS-CoV-2 infection, with these symptoms lasting for at least 2 months with no other explanation. Several studies indicate that around 10% of people recovering from COVID-19 are affected by LC [9]. On the other hand, post-influenza follow-up studies have revealed the prevalence of chronic pulmonary, cardiovascular, and neurological sequelae following the resolution of acute illness in certain patient groups [10–15] as well as post-flu bacterial secondary infection and super-infection [16]. Comparisons between post-COVID and post-flu sequelae were addressed in a cohort of elderly patients, finding similar prevalence, but notable differences in symptomatology [17]. Interestingly, another study described that post-COVID patients developed neuropsychiatric manifestations more quickly, were older, and had more extreme laboratory values than flu patients, underscoring the likely neurotropism of SARS-CoV-2 infection, resulting in new significant neurological and neuropsychiatric sequelae among survivors regardless of COVID-19 disease severity [18].

However, the physiopathology of these diseases is still unknown, although a participation of the immune system is suspected [7]. As a result, scientific and clinical evidence is evolving on the post-acute and long-term effects of COVID-19, which can affect multiple organ systems [19]. Several reports show that LC/post-COVID patients had systemic inflammation and immune dysregulation, as well as significant changes in classical subsets among total $CD4^+$ T cells, specifically a significantly higher proportion of $CD4^+$ Tcm, Tfh, and Treg cells

[20]. Furthermore, differences in other immune cell populations, such as $CD56^{++}$ NK cells, granulocytes, low-density granulocytes, and tissue-homing $CXCR3^+$ monocytes, were found to be significantly increased in convalescents 3 months after infection [8, 21, 22]. In the context of post-influenza infection, studies on alterations in immune cell frequencies and phenotypes are scarce. However, research in mice has detected transcriptionally active influenza A RNA in sites of previous infection. Notably, the persistence and progression of lung damage were found to be partly dependent on IL-13, suggesting sustained Type II immune signaling [23].

Nevertheless, it is still unknown whether these persistent immune alterations are a general mechanism following different viral infections, or whether they are related to disease severity and/or subsequent post-syndrome development or viral reactivation susceptibility. Moreover, it is also unknown whether these post-infection immune alterations are disease-specific or are also induced by other respiratory infections. To date, and to the best of our knowledge, no studies have specifically compared the immune landscape 3 months after primary infection in post-COVID and post-flu patients. Hence, we aimed to characterize the circulating cellular immunome of both post-COVID-19 and post-influenza patients using a deep immunophenotyping of PBMC by mass cytometry (CyTOF) 3 months after diagnose, compared to a cohort of prepandemic healthy controls. Our study addresses a critical knowledge gap by examining immunophenotyping in the context of recovery from SARS-CoV-2 and influenza infections. Our findings reveal specific immunological patterns in post-COVID-19 patients, shedding light on distinctive immune mechanisms that come into play following these infections, providing potential novel therapeutic opportunities.

## 2 | Methods

### 2.1 | Ethics Statement

Participants for the three study cohorts were selected from different clinical studies. One cohort consisted of adult post-COVID-19 patients discharged after hospitalization as standard of care from Hospital Clínico Universitario and Hospital Universitario Río Hortega, both in Valladolid, Spain. Study procedures were medically and ethically approved by the Local Ethics Committee from Valladolid Este, Spain (PI 21-2098). Another cohort consisted of post-influenza patients selected from the influenza arm of the controlled longitudinal, parallel group study Immfact (NL46795.094.13), conducted by the National Institute for Public Health and the Environment (RIVM), Bilthoven, the Netherlands. The Immfact study was approved by the accredited independent Medical Ethics Review Board

METC UMC Utrecht. A cohort of prepandemic healthy donors was selected from the Spanish Network of Biobanks. All participants provided written informed consent before the study procedures. All studies were conducted in compliance with the principles of the Declaration of Helsinki.

## 2.2 | Study Participants and Sample Collection

Venous blood samples were collected from 93 unvaccinated patients who were hospitalized between March and April 2020 at Hospital Clínico Universitario and Hospital Universitario Río Hortega, both in Valladolid (Spain), due to SARS-CoV-2 infection (confirmed by positive RT-PCR), 3 months after hospital discharge (post-COVID). According to Rambaut et al. [24], the SARS-CoV-2 variant circulating during that period belonged to lineage "A", which was present between February 26 to April 27, 2020. Additionally, venous blood samples were collected from a second cohort of 25 post-influenza patients, who were infected with H1N1 or H3N2 influenza virus variants, and were recruited between February 2016 and May 2017, 3 months after laboratory-confirmed (positive RT-PCR) influenza infection (post-flu). Furthermore, blood samples were collected from 25 pre-pandemic healthy donors (HD) from the Spanish Network of Biobanks. Importantly, neither of these two latter cohorts had never been exposed to SARS-CoV-2.

From post-COVID-19 patients and HD, 10 mL of peripheral blood was collected in LH Lithium Heparin Separator tubes. Samples were immediately centrifugedon Ficoll-Paque PLUS (Cytiva) gradient to obtain peripheral blood mononuclear cells (PBMC), which were cryopreserved in duplicates in freezing medium (90% FBS + 10% DMSO) until use. From post-influenza patients, peripheral blood samples were collected in vacutainer cell preparation (CPT) tubes (BD Biosciences, San Jose, CA, USA), and PBMC were isolated according to the manufacturer's instructions and cryopreserved in freezing medium (30% FBS + 10% DMSO) at −135° until testing.

Demographic and clinical information of COVID-19 patients 3 months after hospital discharge were collected, including persistent symptoms related to COVID-19 infection (mainly dyspnea, asthenia and headache, but also heart palpitation, muscle weakness, hair loss, coughs), as well as their clinical data during acute infection, such as oxygen requirement, hospitalization time and treatment received. In addition, clinical and demographic data were also obtained from the post-flu and prepandemic controls. Demographic and clinical information is summarized in Table 1.

## 2.3 | Antibody Cocktail Preparation

The antibody cocktail was designed to complement Maxpar Direct Immune Profiling Assay tubes (MDIPA, Standard Biotools) containing a lyophilized antibody cocktail (Supporting Information S1: Table S1). This panel was supplemented with 10 additional markers (Supporting Information S1: Table S2). Most of the latter antibodies were obtained in a purified form

and conjugated to metals using Maxpar Metal-labeling kits following the manufacturer's instructions (Standard Biotools). Antibodies were titrated in all cases to determine optimal concentration under the same conditions as the tested samples. To minimize experimental variation and promote data consistency, a concentrated antibody cocktail pool was prepared, aliquoted, and stored at −80°C until the day of the staining, as previously described [25].

## 2.4 | Cell Staining and CyTOF Acquisition

Cryopreserved PBMC were thawed at 37°C and transferred to 3 mL of RPMI (Gibco) supplemented with 25 U/mL benzonase (ThermoFisher). RPMI-benzonase was added for a total of 10 mL. Cells were centrifuged at 400$g$ for 5 min and resuspended in 1 mL of Cell Staining Buffer (CSB, Standard Biotools) supplemented with 2 mM EDTA (Invitrogen). Viability and cell count were determined, and $2 \times 10^6$ cells were washed with 1 mL of CSB + EDTA in 5 mL polystyrene round-bottom tubes. Pellets were resuspended in 25 μL of 20 μg/mL of FcR-blocking solution (BD Biosciences) diluted in CSB + EDTA and incubated for 10 min at room temperature (RT). Then, samples were stained by adding 25 μL of the previously described 10-plex antibody cocktail and incubated for 30 min at RT. MDIPA tubes were resuspended in 105 μL of CSB + EDTA. 50 μL of resuspended MDIPA was added to samples stained with the antibody cocktail and further incubated for 30 min at RT. After washing with 1 mL of CSB + EDTA at 400$g$ for 5 min, cell pellets were resuspended in 1 mL of 1.6% PFA (Thermo Scientific) in Maxpar PBS (Standard Biotools), and samples were fixed for 10 min at RT. Finally, samples were centrifuged at 800$g$ for 10 min, and the cell pellets were stained overnight with 500 μL of 5 μM Cell-ID intercalator Ir (Standard Biotools) in Fix and Perm Buffer (Standard Biotools). The next day, samples were stored at −80°C until the day of acquisition.

For CyTOF acquisition, samples were thawed and washed at 800 $g$ for 5 min with 2 mL of CSB. Then, pellets were washed twice with 2 mL of Maxpar Cell Acquisition Solution (CAS, Standard Biotools) at 800 $g$ for 5 min. Cell pellets were resuspended at $8 \times 10^5$–$1 \times 10^6$ cells/mL in CAS together with 0.1x EQ Four Element Calibration Beads (Standard Biotools), and acquired in a CyTOF2/Helios device (Standard Biotools) using a wide-bore sample injector and CyTOF Software version 6.7.1016. The flow rate was set below 400 events/s, and the whole tube was acquired.

## 2.5 | Mass Cytometry Data Normalization and Analysis

After acquisition, fcs files were normalized using the calibration beads and Matlab Normalizer v0.3 [26]. Normalized.fcs files were cleaned up using Maxpar Pathsetter software (Standard Biotools). The default clean-up probability state modeling (PSM) model was used for the identification of intact live singlet cells. Cleaned.fcs files were then uploaded to FlowJo 10.7.2 for further analysis.

**TABLE 1** | Patient description. Demographic and clinical data of post-COVID, post-flu individuals, and pre-pandemic healthy donors.

**Study participants**

| | Post-COVID ($n = 93$) | Post-flu ($n = 25$) | Pre-pandemic controls (HD) ($n = 25$) |
|---|---|---|---|
| Gender | | | |
| Male | 55 (59%) | 11 (44%) | 13 (52%) |
| Female | 38 (41%) | 14 (56%) | 12 (48%) |
| Age | 67 (23–95) | 62 (27–85) | 60 (39–65) |
| Time from acute infection (days) | 80.5 (17–130) | 79 (49–134) | — |
| Hospitalization (days) | 12 (1–55) | 0 (0–5) | — |
| Time from hospital discharge (days) | 70 (10–115) | — | — |
| $O_2$ requirement[a] | | | |
| No | 43 (46%) | — | — |
| Yes | 49 (54%) | — | — |
| Treatment | | | |
| No | 2 (2%) | — | — |
| Antivirals[b] | 77 (83%) | — | — |
| Antibiotics[c] | 77 (83%) | | |
| Corticosteroids | 58 (62%) | — | — |
| Immunomodulators[d] | 82 (88%) | — | — |
| Long COVID | | — | — |
| No | 66 (71%) | — | — |
| Yes | 23 (29%) | — | — |

*Note:* Data are listed as median (range) or numbers (%).

[a] For oxygen requirement, "no" is defined as no need for oxygen, while "yes" is defined as the need for masks, non-invasive mechanical ventilation, or invasive mechanical ventilation to supply oxygen.

[b] Antivirals administered were lopinavir in combination with ritonavir.

[c] Antibiotic used was azithromycin.

[d] Immunomodoluators considered were hydroxychloroquine, betaferon, cyclosporine, colchicine, and tocilizumab.

## 2.6 | Statistical Analysis

Mass cytometry data of every individual were integrated into a single database. To use the most relevant features, we selected those with a variation coefficient (CV) higher than 0.5 among all the individuals of the study, and MSI with values > 10 in at least 5% of individuals (Supporting Information S1: Tables S3 and S4). The selected features were log2-transformed and then scaled and centered using the R scale function. Principal Component Analysis (PCA) of scaled features was performed using factoMineR and factoextra R packages. The top-50 features that showed the highest contribution to components 1 and 2 of the PCA were selected for clustering and classification models (Supporting Information S1: Figure S1). Before clustering analysis, the elbow method was performed to determine the optimal number of clusters (Supporting Information S1: Figure S2). K-means clustering of patients was performed using the scaled features and the stats R package, with 4 centers and 100 iterations. Heatmap representations were performed using the Complex Heatmap R package, and bar and scatter plots were done using ggplot2 R package. Random forest and logistic regression classification models were evaluated using Orange Data Mining software [27]. For the construction of the diagnosis prediction model, our cohort of individuals was split into a training set (75% of individuals,

$n = 108$) and a testing set (25% of individuals, $n = 35$) according to their diagnose. A 10-fold cross-validation was run on the training set. For logistic regression, we used Lasso regularization type with $C = 1$, while for random forest, 10 trees and 3 as the smallest subset were set. A receiver operating characteristic (ROC) curve was performed to evaluate the model's predictive ability, and the area under the curve (AUC) was used as an evaluation index. Afterwards, the model was applied to the testing set to predict the diagnosis of the individuals. Statistical analyses were performed using R. Comparisons of continuous values were assessed using Mann–Whitney $t$-test. Comparisons of categorical values were calculated using Fisher's Exact Test. A $p$-value of $< 0.05$ was considered statistically significant.
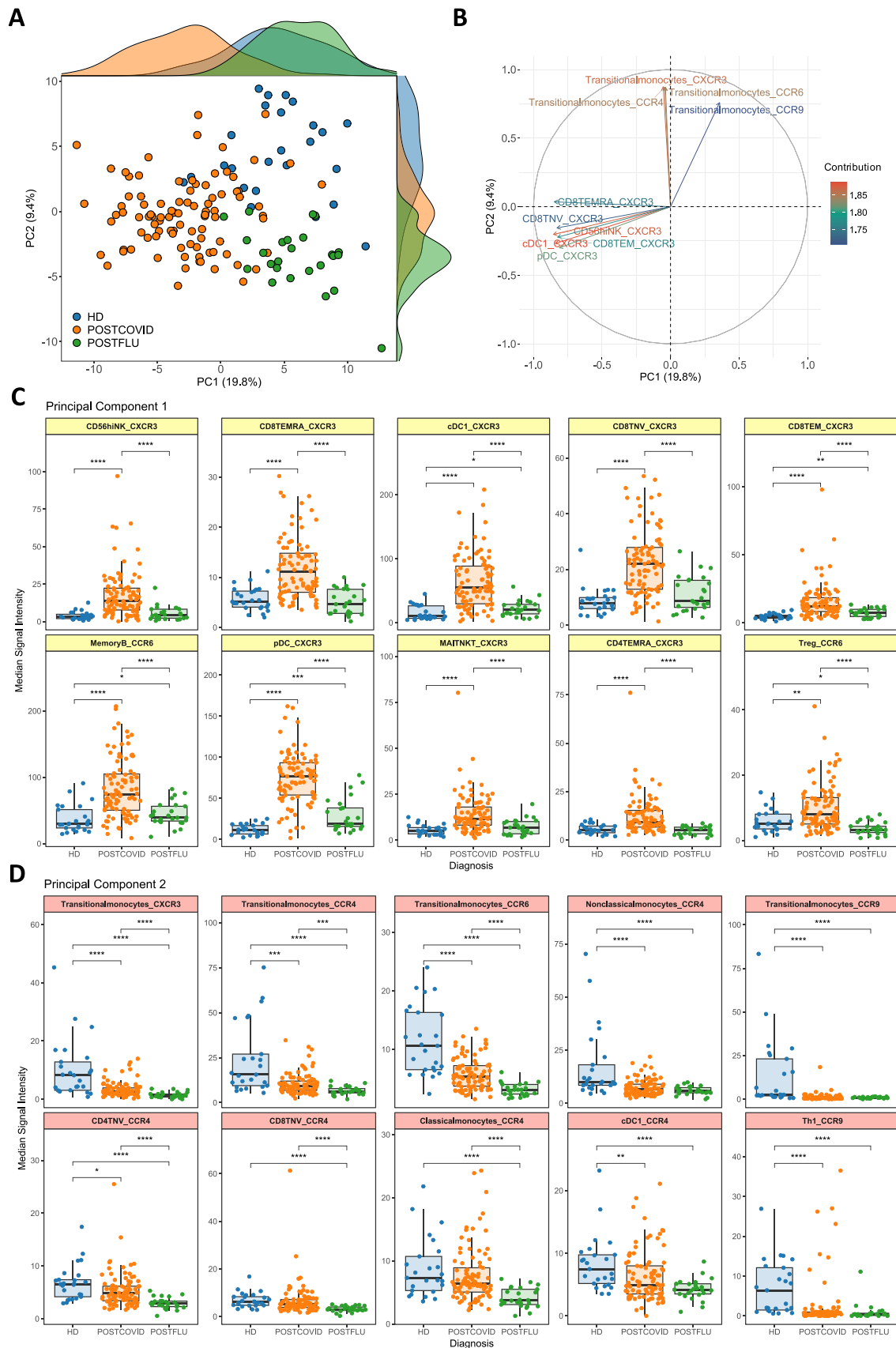
## 3 | Results

### 3.1 | Altered Migratory Profile of Post-COVID and Post-Flu Patients

To identify whether COVID-19 patients display unique immune alterations following SARS-CoV-2 infection, or whether, on the contrary, these are also induced by other

respiratory infections, we assessed the circulating cellular immunome of COVID-19 patients 3 months after hospital discharge, and compared them with a cohort of post-flu patients (matched for sex, age and time since first infection) as well as a cohort of healthy pre-pandemic controls. Figure 1 shows the gating strategy used to identify, in each individual, a total of 43 different immune cell subsets. In addition, the median signal intensities (MSI) of 16 different functional markers (CCR2, CCR4, CCR5, CCR6, CCR7, CCR9, CXCR1, CXCR3, CXCR5, CD25, CD38, CD57, CD147, CD161, CD62L, and HLA-DR) were determined within each immune subset. Cell frequencies, referred to as total live cells, and MSI within each subset, were extracted and exported to csv files for further analyses.

Having obtained all the CyTOF features in all the individuals, we first performed a PCA analysis, which revealed a differential immune fingerprint among the three studied cohorts (Figure 2A). Indeed, post-COVID patients were clustered apart from the other cohorts based on component 1 (19.8%), while both post-flu and prepandemic controls were more alike as they mainly differed on component 2 (9.4%). Next, we aimed to identify the most important features contributing to such variability. Our results revealed that within the 141 most variable features, 34 of them reflected alterations in the proportion of circulating cell subsets (Supporting Information S1: Table S3), while 107 were related to the MSI levels of the studied functional markers within a given immune subset (Supporting Information S1: Table S4). Once they were ordered, the 10 features with the highest impact of the PCA (Figure 2B) were the expression of CCR4, CCR6, and CCR9

by transitional monocytes, together with the expression of the chemokine receptor CXCR3 by CD56$^{hi}$ NK cells, type 1 conventional dendritic cells (cDC1), CD8$^+$ naïve, CD8$^+$ effector memory and CD8$^+$ effector memory CD45RA$^+$ T cells, plasmacytoid dendritic cells (pDC), and transitional monocytes.

We next identified the 10 most important features specifically contributing to both components 1 and 2 of the PCA. Figure 2C represents the expression levels of both CXCR3 and CCR6 by the different subsets contributing (from more to less) to component 1 of the PCA, revealing how post-COVID patients display an increased expression of these chemokine receptors involved in lymphoid migration compared to both pre-pandemic controls and post-influenza patients. Besides, some of these alterations were also found in the latter when compared to the controls, although at much lower extent. Component 2 (Figure 2D) was mainly influenced by the expression of several chemokine receptors (CXCR3, CCR4, CCR6, and CCR9), showing them from more to less contribution. However, their expression was mainly related to myeloid cells, which had a reduced expression in post-flu patients and, to a lesser extent, in post-COVID patients compared to healthy controls.

Of note, and although there were some differences among the three studied cohorts on the circulating levels of different immune cell subsets (data not shown), their contribution was, however, much lower than that elicited by the differential migratory profile of the immune subsets (Figure 2C,D) since the most prominent one (circulating levels of CD8$^+$ TEMRA T-cells) was not found until the sixth



**FIGURE 1** | Identification of immune cell subsets by mass cytometry. Representative mass-cytometry plots showing the hierarchical gating strategy used for the identification of immune cell populations and their subsets.

**FIGURE 2** | Post-COVID and post-flu immune fingerprint. (A) Principal component analysis (PCA) of post-COVID (orange), post-flu (green), and healthy donors (HD, blue) based on mass cytometry data. (B) Biplot of the top 10 features that contributed the most to PCA. The colors in the plot represent the contribution (in percentage) for each feature, varying from blue (lower contribution) to red (higher contribution). Box plots of the 10 features contributing to both component 1 of PCA (C) and component 2 (D) are shown. Mann–Whitney test was applied. $p$-values $< 0.05$ were considered as statistically significant (*$p < 0.05$, **$p < 0.01$, ***$p < 0.001$, ****$p < 0.0001$).

feature contributing to the third component of the PCA (Supporting Information S1: Figure S3).

## 3.2 | Identification of Specific Post-Respiratory Infection Signatures

Since both post-COVID and post-flu displayed a differential expression of migratory markers compared to pre-pandemic controls, we next aimed to develop a model to predict patient classification. To that end, we used the top 50 features with the highest contribution to both components 1 and 2 of the PCA (Supporting Information S1: Figure S1). Results from both random forest and logistic regression models are shown in Table 2, revealing that the AUCs were over 0.95 in both the training (Figure 3A) and the testing set (Figure 3B). Furthermore, both models exhibited outstanding scores to classify new individuals, as both showed a classification accuracy (CA) over 0.90. Hence, these results confirm the presence of a persistent and differential immune disturbance on the migratory profile of circulating mononuclear cells up to 3 months following post-COVID and post-influenza infection.

## 3.3 | Unsupervised Clustering Reveals Two Immunological Groups of Post-COVID Patients

We also performed an unsupervised classification of all the individuals based on their mass cytometry immunological features, regardless of their diagnosis, using the K-means clustering algorithm. As before, the top 50 features contributing to components 1 and 2 of the PCA were used (Supporting Information S1: Figure S1). The elbow method determined, from the total of individuals, an optimal number of 4 clusters to classify all the observed biological variability (Supporting Information S1: Figure S2 and Figure 4). Cluster 1 was mainly composed of healthy donors ($n = 15$), together with 6 post-COVID patients. Cluster 3 was enriched in post-flu patients ($n = 24$), although it also included 4 healthy donors and 4 post-COVID. On the other hand, clusters 2 and 4 consisted of almost exclusively post-COVID patients ($n = 37$ and $n = 46$, respectively). In cluster 2, one healthy donor was found, while cluster 4 included one post-flu and five healthy donors (Figure 4).

In addition, 4 modules of features were observed according to the hierarchical clustering indicating grouped regulation of immune parameters in the patients. Module 1 consisted mostly of the expression of chemokine receptors CXCR3 and CCR6 by lymphoid cells, together with the expression of CCR2 by DC. Likewise, module 2 was made of lymphoid cells expressing CD62L or CXCR2, together with the expression of CXCR5 by naïve B cells. Module 3 was, however, more heterogeneous regarding the expression of several chemokine receptors (CCR6, CCR4, CCR9, and CXCR3) by myeloid cells as well as the expression of CCR9 by $CD4^+$ type 1 helper T cells. Last, module 4 consisted of several immune subsets expressing CCR4, together with $CCR6^+$ plasmablasts and $CD4^+$ central memory T cells.

Notably, patients from cluster 2 (mainly made of post-COVID patients) displayed an increased expression of both modules 1 and 2 as compared to the other clusters, including cluster 4, which was the other post-COVID-bearing cluster. Likewise, modules 1 and 2 were quite similar between clusters 1 (mainly prepandemic controls) and 3 (mainly post-flu patients). Of note, cluster 4 (mainly post-COVID patients) had a transitional state, in both modules 1 and 2, referred to clusters 1 (mainly controls) and 3 (mainly post-flu) (Supporting Information S1: Figures S4 and S5). As for cluster 1 (mainly pre-pandemic controls), its main difference with the other clusters relied on module 3, which was increased (Supporting Information S1: Figure S6). Similarly, cluster 3 (mainly post-flu patients) showed a decrease in expression in module 4 compared to cluster 4 (mainly post-COVID patients) (Supporting Information S1: Figure S7).

As our data indicate a level of diversity within the group of post-COVID patients in contrast to pre-pandemic healthy controls and post-flu patients (Figure 4), we next aimed to identify the factors underlying such diversity including gender and age at diagnose, as well as disease severity (considered as both days in hospital or oxygen requirement), treatment during infection, or subsequent development of long-COVID (Figure 5). Of note, and although the proportion of patients who have subsequently developed long COVID was slightly enriched in cluster 2, that was, however, not statistically significant (Figure 5F). Thus, separation of the post-COVID patients into two immune clusters could only be explained by

**TABLE 2** | Logistic regression and Random Forest.

| Training Set: Scores Model | TP | TN | FP | FN | AUC | CA | F1 | Precision | Recall | Specificity |
|---|---|---|---|---|---|---|---|---|---|---|
| Logistic regression | 103 | 211 | 5 | 5 | 0.99 | 0.95 | 0.95 | 0.96 | 0.95 | 0.97 |
| Random forest | 99 | 207 | 9 | 9 | 0.97 | 0.92 | 0.91 | 0.92 | 0.92 | 0.91 |

| Testing Set: Scores Model | TP | TN | FP | FN | AUC | CA | F1 | Precision | Recall | Specificity |
|---|---|---|---|---|---|---|---|---|---|---|
| Logistic regression | 34 | 69 | 1 | 1 | 0.99 | 0.97 | 0.97 | 0.98 | 0.97 | 0.99 |
| Random forest | 33 | 68 | 2 | 2 | 0.98 | 0.94 | 0.94 | 0.95 | 0.94 | 0.94 |

*Note:* Performance metrics of logistic regression and random forest models for the prediction of diagnosis using the top-50 features of PCA components 1 and 2 in the training (above) and testing set (bottom). Scores of both models include classification accuracy (CA), F1 score, precision, recall, and specificity. TP: true positive, TN: true negative, FP: false positive, FN: false negative.
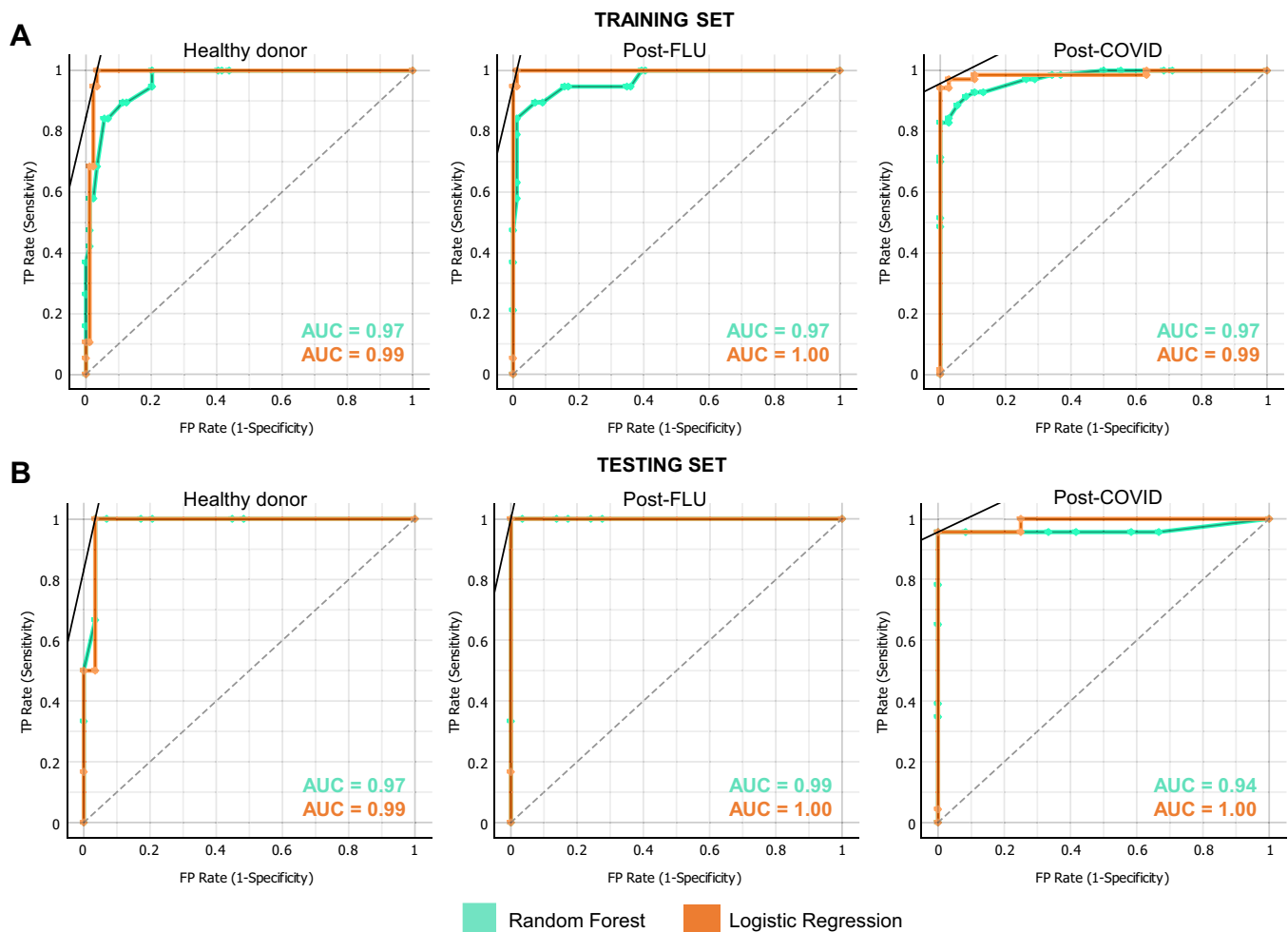
**FIGURE 3** | Patient classification. Receiver operating characteristic (ROC) curves of logistic regression (orange) and random forest (turquoise) models for each of the predicted classes using (A) the training and (B) the testing set. The area under the curve (AUC) value of each model is annotated in each graph. The dashed line indicates a random prediction.

age (Figure 5A) and did not relate to subsequent long-COVID development (Figure 5F), gender (Figure 5C), disease severity (Figure 5B,D), or treatment during hospitalization (Figure 5E).

## 4 | Discussion

Over the past 4 years, extensive research has delved into how the immune system interacts with SARS-CoV-2 and the nature of immune responses following infection. However, there is limited information regarding whether SARS-CoV-2 infection can induce relatively prolonged perturbations of immune cell subsets, and if these perturbations are specific for this disease. To address this gap, we conducted a comprehensive analysis of the cellular immunome in post-COVID patients alongside post-flu patients, 3 months after infection. Our objective was to determine whether the underlying immunological mechanisms of both infections exhibit similarities or differences. Understanding these immune signatures post-infection could offer insights into the pathogenesis of COVID-19 and inform strategies for patient management. Additionally, exploring the similarities and differences between post-COVID and post-influenza immune cell subsets may unveil common

mechanisms of viral clearance and immune modulation, facilitating the development of broad-spectrum antiviral therapies or immunomodulatory interventions. Building from that, we hereby have shown, for the first time to our knowledge, that respiratory infections (both post-COVID and post-flu) induce specific alterations of immune cell subsets, which are maintained over time. However, those alterations are much more prominent in the case of post-COVID patients, especially in younger patients.

Severe acute COVID-19 is marked by the release of different inflammatory mediators at infection sites, such as interleukins and chemokines, by recruited inflammatory immune cells through chemokine receptors, which can mediate the cytokine storm syndrome in severe patients [28]. Several studies have shown that chemokine receptors are key players in the immune response to COVID-19. Hence, CXCR3 migration through CXCL10 binding has important roles in the recruitment of selective cells to inflamed sites [29], so this axis may be one of the key mediators causing dysregulation of immune responses in COVID-19 [30, 31]. Indeed, CXCR3 over-expression, which has been associated with pulmonary conditions such as pulmonary fibrosis [32], is upregulated on T cells and NK cells in COVID-19 patients, allowing its
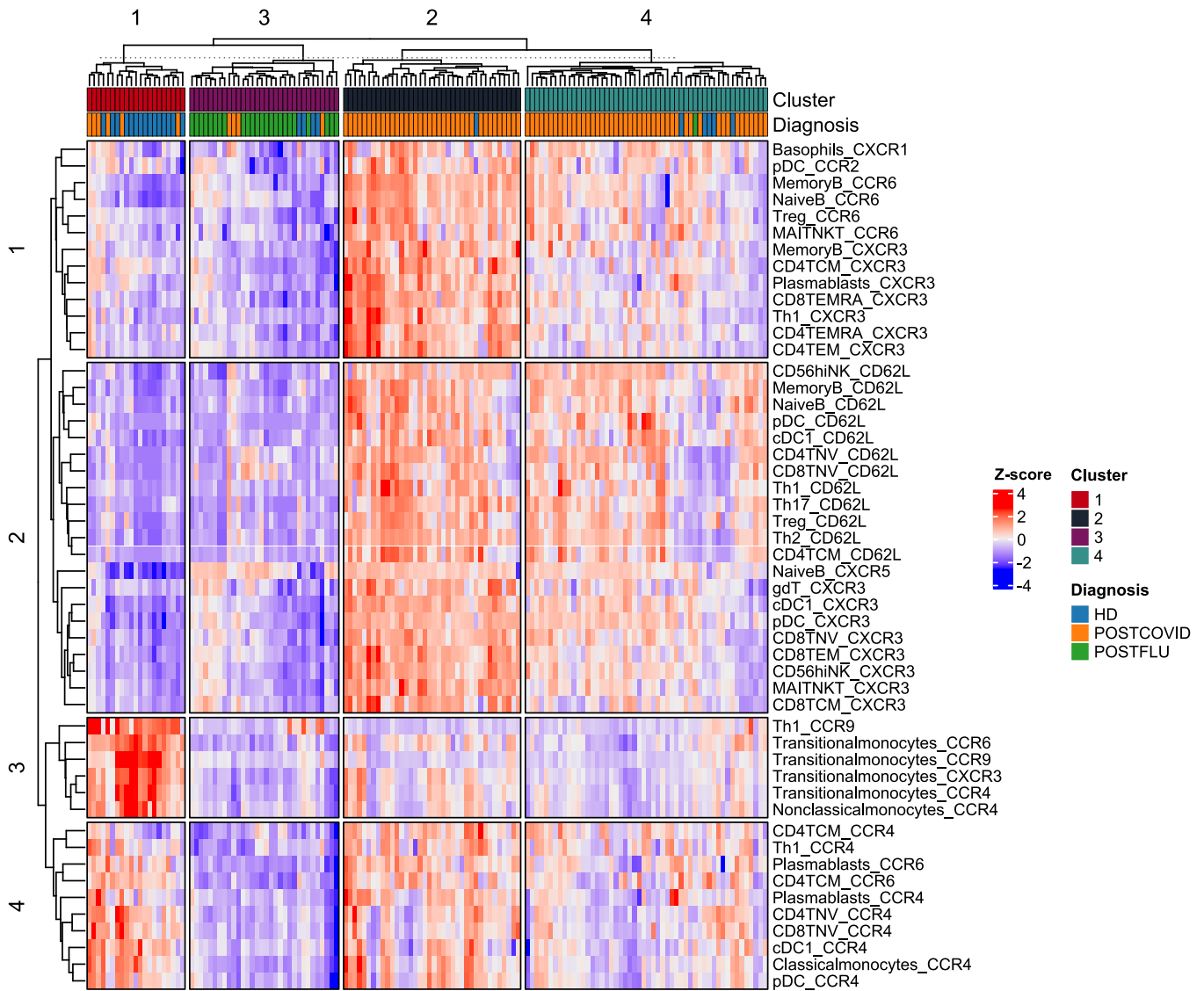
**FIGURE 4** | Unsupervised clustering reveals two immunological groups of post-COVID patients. The heatmap is a representation of selected features across all individuals. The colors in the heatmap represent the Z-score for each feature, varying from blue (lower expression) to red (higher expression). The features used for the analysis are shown in rows and split into modules according to the dendrogram on the left, which represents the hierarchical similarity between features (euclidean distance, complete method). In columns, each individual is shown together with it diagnose (healthy donors in blue, post-COVID in orange and post-flu in green) and split according to cluster data (cluster 1 in red, cluster 2 in navy blue, cluster 3 in purple and cluster 4 in cyan) above the heatmap (euclidean distance, complete method).

migration to the lungs where the virus primarily replicates [30, 33]. In a similar manner, Saris et al. [34] found a higher expression of CCR4 on circulating T cells from COVID patients in intensive care units (ICU) compared to non-ICU patients. Additionally, there is an enrichment of CCR6+ cytotoxic T-cells in the bronchoalveolar aspirate of mechanically ventilated COVID-19 patients. SARS-CoV-2 has also been found to increase the expression of CCR2 and CCR5 in the human thoracic dorsal root ganglion, suggesting the influence of inflammatory mediators in activating sensory neurons associated with the lungs [35]. Furthermore, there is a significant positive correlation between the frequency of CCR5 Δ32 and COVID-19 infection and mortality rate [36]. Besides, the expression of chemokine receptors CCR6 and CXCR3 has been associated with lung-resident lymphocytes [37], indicating a persistent respiratory tropism in post-COVID patients even

3 months after the resolution of the symptomatic infection. Moreover, CXCR3 results in exacerbated lung inflammation and impaired immune responses against viruses, including influenza [30, 33]. In addition, NK cells can facilitate inflammation during viral infections [38]. Thus, increased expression of lung-homing chemokines and chemokine receptors on NK cells, effector T CD4+, together with CD8+, and memory B cells, among others, may facilitate cell migration and exacerbate lung inflammation in COVID-19. All in all, these results and the observations in our present study suggest that post-COVID patients have persistent alterations in the chemotactic profile of the lymphoid compartment and a moderate effect in the myeloid cells, still 3 months after hospital discharge.

Having said that, only a fraction of these alterations were COVID-specific, since changes in the migratory profile were
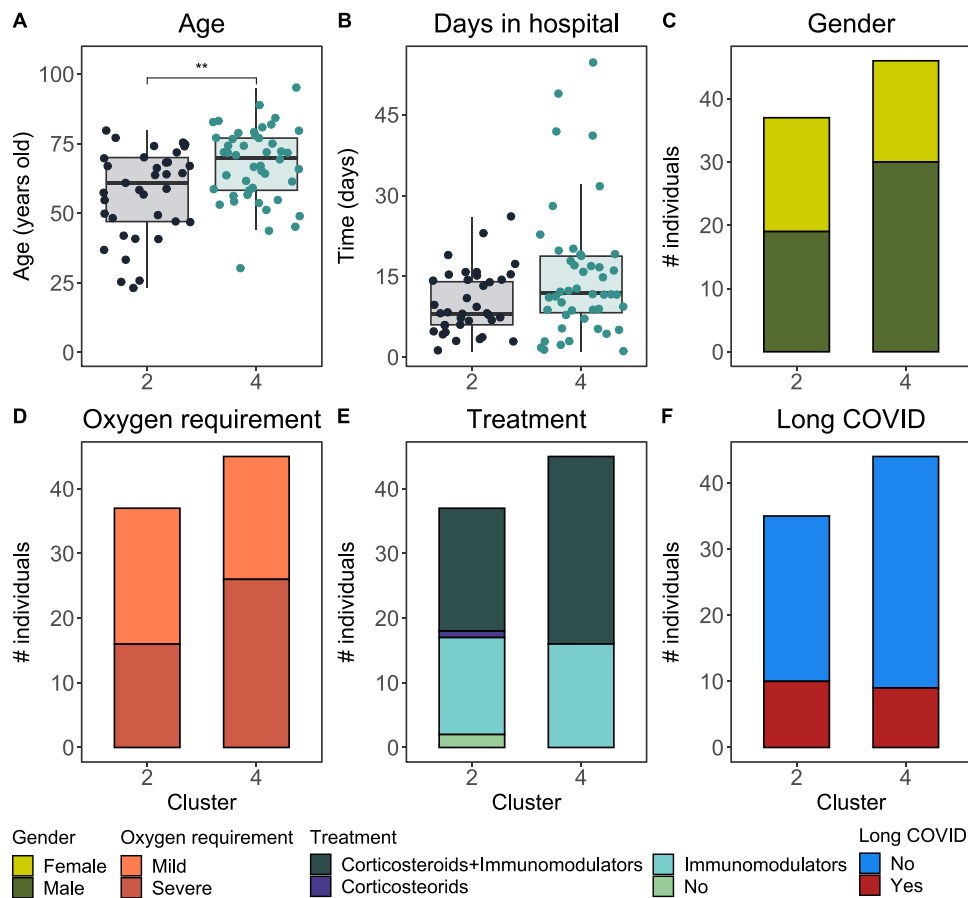
**FIGURE 5** | Clinical parameters within the two immunological groups of COVID-19 patients. Post-COVID patients within clusters 2 and 4 of K-means were compared based on their (A) age at COVID-19 diagnose and (B) subsequent hospitalization days, (C) gender, (D) oxygen need during hospitalization, (E) treatment, or (F) subsequent development of Long-COVID. Mann–Whitney test was applied, and $p < 0.05$ was considered statistically significant (**$p < 0.01$).

also found in post-flu patients. CXCR3 and CCR6 axis upregulation in lymphoid cells was specifically associated with post-COVID patients, while downregulation of CCR4 and CCR9 was found in both post-COVID and post-flu patients, while more intense in the latter. The finding that this altered leukocyte trafficking profile is maintained over time, even months after infection, seems to reflect the natural course of infection, which would then diverge between SARS-CoV-2 and influenza virus infection. Indeed, it has now become clear that SARS-CoV-2 infection, as opposed to either respiratory virus like influenza, is multisystemic, affecting many tissues (e.g., brain, kidney, gut etc.) aside of the lungs [39]. Hence, the increased chemokine receptor levels found in post-COVID patients might be explained by these multisystemic effects, which also translate into a much higher degree of variability in these patients, as referred to post-influenza ones. Besides, neither subsequent LC development, gender, nor disease severity during infection was the cause of such variability, which was driven by a differential age at first diagnose. Our findings indicate that younger post-COVID patients exhibit a stronger migratory activation profile on mainly lymphoid cells compared to older individuals, suggesting that immune recovery trajectories may differ across age groups [40]. Hence, immune differences among both post-COVID groups could be related to the mechanisms of immune senescence.

It is worth noting that in the present study, we have performed a descriptive analysis and only the immune profile of these patients was assessed, but other factors could contribute to the heterogeneity of post-COVID patients and the association with LC symptoms, such as genetics or co-infections. For example, differences in HLA alleles have been associated with viral clearance capacity, suggesting that individuals with low-affinity HLA for SARS-CoV-2 antigens may experience prolonged viral persistence and increased susceptibility to LC [41]. Additionally, genetic polymorphisms in VEGFR-2 have been identified as modulators of COVID-19 severity in an age- and sex-dependent manner [40], and genetic predisposition to mitochondrial dysfunction and altered cellular energy capacity have also been postulated as potential contributors to LC [42]. On the other hand, bacteria and virus co-infections have also been reported to significantly worsen COVID-19 severity and increase LC risk [43–46]. Nevertheless, our findings reinforce the idea that post-COVID immune responses are heterogeneous, and therefore, the integration of genetic and functional studies in future research could help to elucidate the mechanisms underlying such heterogeneity of post-COVID individuals.

In summary, we have described that following a viral respiratory infection, changes in the chemokine receptor profile

can be found still 3 months after disease recovery. Besides, we have also proved that such immune features are different in post-influenza and post-COVID patients after disease recovery, being more prominent in the latter and more pronounced in younger individuals. Understanding the factors driving these changes may, therefore, highlight differences in immune recovery from various respiratory infections.

## Conflicts of Interest

The authors declare no conflicts of interest.

## Data Availability Statement

The data that support the findings of this study are available from the corresponding author upon reasonable request.

## References

1. M. Wiech, P. Chroscicki, J. Swatler, et al., "Remodeling of T Cell Dynamics During Long COVID Is Dependent on Severity of SARS-CoV-2 Infection," *Frontiers in Immunology* 13 (2022): 886431, https://doi.org/10.3389/fimmu.2022.886431.

2. P. Moss, "The T Cell Immune Response Against SARS-CoV-2," *Nature Immunology* 23, no. 2 (2022): 186–193, https://doi.org/10.1038/s41590-021-01122-w.

3. G. Chen, D. Wu, W. Guo, et al., "Clinical and Immunological Features of Severe and Moderate Coronavirus Disease 2019," *Journal of Clinical Investigation* 130, no. 5 (2020): 2620–2629, https://doi.org/10.1172/JCI137244.

4. P. Taeschler, S. Adamo, Y. Deng, et al., "T-Cell Recovery and Evidence of Persistent Immune Activation 12 Months After Severe COVID-19," *Allergy* 77, no. 8 (2022): 2468–2481, https://doi.org/10.1111/all.15372.

5. J. Y. H. Kim, M. Ragusa, F. Tortosa, et al., "Viral Reactivations and Co-Infections in COVID-19 Patients: A Systematic Review," *BMC Infectious Diseases* 23, no. 1 (2023): 259, https://doi.org/10.1186/s12879-023-08117-y.

6. I. Martín-Loeches, A. Sanchez-Corral, E. Diaz, et al., "Community-Acquired Respiratory Coinfection in Critically Ill Patients With Pandemic 2009 Influenza A(H1N1) Virus," *Chest* 139, no. 3 (2011): 555–562, https://doi.org/10.1378/chest.10-1396.

7. C. Tackey, P. M. Slepian, H. Clarke, and N. Mittal, "Post-Viral Pain, Fatigue, and Sleep Disturbance Syndromes: Current Knowledge and Future Directions," *Canadian Journal of Pain* 7, no. 2 (2023): 2272999, https://doi.org/10.1080/24740527.2023.2272999.

8. F. J. Ryan, C. M. Hope, M. G. Masavuli, et al., "Long-Term Perturbation of the Peripheral Immune System Months After SARS-CoV-2 Infection," *BMC Medicine* 20, no. 1 (2022): 26, https://doi.org/10.1186/s12916-021-02228-6.

9. M. Santopaolo, M. Gregorova, F. Hamilton, et al., "Prolonged T-Cell Activation and Long Covid Symptoms Independently Associate With Severe COVID-19 at 3 Months," *eLife* 12 (2023): e85009, https://doi.org/10.7554/eLife.85009.

10. S. Toovey, S. S. Jick, and C. R. Meier, "Parkinson's Disease or Parkinson Symptoms Following Seasonal Influenza," *Influenza and Other Respiratory Viruses* 5, no. 5 (2011): 328–333, https://doi.org/10.1111/j.1750-2659.2011.00232.x.

11. C. E. Luyt, A. Combes, M. H. Becquemin, et al., "Long-Term Outcomes of Pandemic 2009 Influenza A(H1N1)-Associated Severe ARDS," *Chest* 142, no. 3 (2012): 583–592, https://doi.org/10.1378/chest.11-2196.

12. W. Liu, L. Peng, H. Liu, and S. Hua, "Pulmonary Function and Clinical Manifestations of Patients Infected With Mild Influenza A Virus Subtype H1N1: A One-Year Follow-Up," *PLoS One* 10, no. 7 (2015): e0133698, https://doi.org/10.1371/journal.pone.0133698.

13. J. Chen, J. Wu, S. Hao, et al., "Long Term Outcomes in Survivors of Epidemic Influenza A (H7N9) Virus Infection," *Scientific Reports* 7, no. 1 (2017): 17275, https://doi.org/10.1038/s41598-017-17497-6.

14. S. A. Sellers, R. S. Hagan, F. G. Hayden, and W. A. Fischer, "The Hidden Burden of Influenza: A Review of the Extra-Pulmonary Complications of Influenza Infection," *Influenza and Other Respiratory Viruses* 11, no. 5 (2017): 372–393, https://doi.org/10.1111/irv.12470.

15. F. Tesch, F. Ehm, F. Loser, et al., "Post-Viral Symptoms and Conditions Are More Frequent in COVID-19 Than Influenza, but Not More Persistent," *BMC Infectious Diseases* 24, no. 1 (2024): 1126, https://doi.org/10.1186/s12879-024-10059-y.

16. M. N. Ballinger and T. J. Standiford, "Postinfluenza Bacterial Pneumonia: Host Defenses Gone Awry," *Journal of Interferon & Cytokine Research* 30, no. 9 (2010): 643–652, https://doi.org/10.1089/jir.2010.0049.

17. K. W. Fung, F. Baye, S. H. Baik, Z. Zheng, and C. J. McDonald, "Prevalence and Characteristics of Long Covid in Elderly Patients: An Observational Cohort Study of Over 2 Million Adults in the US," *PLoS Medicine* 20, no. 4 (2023): e1004194, https://doi.org/10.1371/journal.pmed.1004194.

18. A. L. Iosifescu, W. S. Hoogenboom, A. J. Buczek, R. Fleysher, and T. Q. Duong, "New-Onset and Persistent Neurological and Psychiatric Sequelae of COVID-19 Compared to Influenza: A Retrospective Cohort Study in a Large New York City Healthcare Network," *International Journal of Methods in Psychiatric Research* 31, no. 3 (2022): e1914, https://doi.org/10.1002/mpr.1914.

19. S. Mehandru and M. Merad, "Pathological Sequelae of Long-Haul COVID," *Nature Immunology* 23, no. 2 (2022): 194–202, https://doi.org/10.1038/s41590-021-01104-y.

20. K. Yin, M. J. Peluso, X. Luo, et al., "Long COVID Manifests With T Cell Dysregulation, Inflammation and an Uncoordinated Adaptive Immune Response to SARS-CoV-2," *Nature Immunology* 25, no. 2 (2024): 218–225, https://doi.org/10.1038/s41590-023-01724-6.

21. M. Koutsakos, L. C. Rowntree, L. Hensen, et al., "Integrated Immune Dynamics Define Correlates of COVID-19 Severity and Antibody Responses," *Cell Reports Medicine* 2, no. 3 (2021): 100208, https://doi.org/10.1016/j.xcrm.2021.100208.

22. B. Kratzer, D. Trapin, P. Ettel, et al., "Immunological Imprint of COVID-19 on Human Peripheral Blood Leukocyte Populations," *Allergy* 76, no. 3 (2021): 751–765, https://doi.org/10.1111/all.14647.

23. S. P. Keeler, E. V. Agapov, M. E. Hinojosa, A. N. Letvin, K. Wu, and M. J. Holtzman, "Influenza A Virus Infection Causes Chronic Lung Disease

Linked to Sites of Active Viral RNA Remnants," *The Journal of Immunology* 201, no. 8 (2018): 2354–2368, https://doi.org/10.4049/jimmunol.1800671.

24. A. Rambaut, E. C. Holmes, Á. O'Toole, et al., "A Dynamic Nomenclature Proposal for SARS-CoV-2 Lineages to Assist Genomic Epidemiology," *Nature Microbiology* 5, no. 11 (2020): 1403–1407, https://doi.org/10.1038/s41564-020-0770-5.

25. A. R. Schulz, S. Baumgart, J. Schulze, M. Urbicht, A. Grützkau, and H. E. Mei, "Stabilizing Antibody Cocktails for Mass Cytometry," *Cytometry, Part A* 95, no. 8 (2019): 910–916, https://doi.org/10.1002/cyto.a.23781.

26. R. Finck, E. F. Simonds, A. Jager, et al., "Normalization of Mass Cytometry Data With Bead Standards," *Cytometry, Part A* 83, no. 5 (2013): 483–494, https://doi.org/10.1002/cyto.a.22271.

27. C. T. Demsar J, A. Erjavec, C. Gorup, et al., "Orange: Data Mining Toolbox in Python," *Journal of Machine Learning Research* 14 (2013): 2349–2353.

28. B. A. Khalil, N. M. Elemam, and A. A. Maghazachi, "Chemokines and Chemokine Receptors During COVID-19 Infection," *Computational and Structural Biotechnology Journal* 19 (2021): 976–988, https://doi.org/10.1016/j.csbj.2021.01.034.

29. M. Gudowska-Sawczuk and B. Mroczko, "What Is Currently Known About the Role of CXCL10 in SARS-CoV-2 Infection?," *International Journal of Molecular Sciences* 23, no. 7 (2022): 3673, https://doi.org/10.3390/ijms23073673.

30. D. Brownlie, I. Rødahl, R. Varnaite, et al., "Comparison of Lung-Homing Receptor Expression and Activation Profiles on NK Cell and T Cell Subsets in COVID-19 and Influenza," *Frontiers in Immunology* 13 (2022): 834862, https://doi.org/10.3389/fimmu.2022.834862.

31. H. Y. Zheng, X. Y. He, W. Li, et al., "Pro-Inflammatory Microenvironment and Systemic Accumulation of CXCR3+ Cell Exacerbate Lung Pathology of Old Rhesus Macaques Infected With Sars-Cov-2," *Signal Transduction and Targeted Therapy* 6, no. 1 (2021): 328, https://doi.org/10.1038/s41392-021-00734-w.

32. D. Jiang, J. Liang, J. Hodge, et al., "Regulation of Pulmonary Fibrosis by Chemokine Receptor CXCR3," *Journal of Clinical Investigation* 114, no. 2 (2004): 291–299, https://doi.org/10.1172/JCI16861.

33. T. Liechti, Y. Iftikhar, M. Mangino, et al., "Immune Phenotypes That Are Associated With Subsequent COVID-19 Severity Inferred From Post-Recovery Samples," *Nature Communications* 13, no. 1 (2022): 7255, https://doi.org/10.1038/s41467-022-34638-2.

34. A. Saris, T. D. Y. Reijnders, M. Reijm, et al., "Enrichment of CCR6(+) CD8(+) T Cells and CCL20 in the Lungs of Mechanically Ventilated Patients With COVID-19," *European Journal of Immunology* 51, no. 6 (2021): 1535–1538, https://doi.org/10.1002/eji.202049046.

35. P. R. Ray, A. Wangzhou, N. Ghneim, et al., "A Pharmacological Interactome Between COVID-19 Patient Samples and Human Sensory Neurons Reveals Potential Drivers of Neurogenic Pulmonary Dysfunction," *Brain, Behavior, and Immunity* 89 (2020): 559–568, https://doi.org/10.1016/j.bbi.2020.05.078.

36. A. K. Panda, A. Padhi, and B. A. K. Prusty, "CCR5 Δ32 Minorallele Is Associated With Susceptibility to SARS-CoV-2 Infection and Death: An Epidemiological Investigation," *Clinica Chimica Acta* 510 (2020): 60–61, https://doi.org/10.1016/j.cca.2020.07.012.

37. H. X. Tan, J. A. Juno, R. Esterbauer, et al., "Lung-Resident Memory B Cells Established After Pulmonary Influenza Infection Display Distinct Transcriptional and Phenotypic Profiles," *Science Immunology* 7, no. 67 (2022): eabf5314, https://doi.org/10.1126/sciimmunol.abf5314.

38. G. Zhou, S. W. W. Juang, and K. P. Kane, "NK Cells Exacerbate the Pathology of Influenza Virus Infection in Mice," *European Journal of Immunology* 43, no. 4 (2013): 929–938, https://doi.org/10.1002/eji.201242620.

39. T. Flerlage, D. F. Boyd, V. Meliopoulos, P. G. Thomas, and S. Schultz-Cherry, "Influenza Virus and SARS-CoV-2: Pathogenesis and Host Responses in the Respiratory Tract," *Nature Reviews Microbiology* 19, no. 7 (2021): 425–441, https://doi.org/10.1038/s41579-021-00542-7.

40. D. B. Sayın Kocakap, S. Kaygusuz, E. Aksoy, et al., "Adverse Effect of VEGFR-2 (rs1870377) Polymorphism on the Clinical Course of COVID-19 in Females and Males in an Age-Dependent Manner," *Microbes and Infection* 25, no. 8 (2023): 105188, https://doi.org/10.1016/j.micinf.2023.105188.

41. A. Georgopoulos, L. James, and P. Peterson, "Human Leukocyte Antigen (HLA) at the Root of Persistent Antigens and Long COVID," *Journal of Immunological Sciences* 9, no. 1 (2025): 1–3, https://doi.org/10.29245/2578-3009/2025/1.1257.

42. K. S. Hansen, S. E. Jørgensen, C. Cömert, et al., "Genetic Landscape and Mitochondrial Metabolic Dysregulation in Patients Suffering From Severe Long COVID," *Journal of Medical Virology* 97, no. 3 (2025): e70275, https://doi.org/10.1002/jmv.70275.

43. A. Alqahtani, E. Alamer, M. Mir, et al., "Bacterial Coinfections Increase Mortality of Severely Ill COVID-19 Patients in Saudi Arabia," *International Journal of Environmental Research and Public Health* 19, no. 4 (2022): 2424, https://doi.org/10.3390/ijerph19042424.

44. B. Baral, V. Saini, M. Kandpal, et al., "The Interplay of Co-Infections in Shaping COVID-19 Severity: Expanding the Scope Beyond SARS-CoV-2," *Journal of Infection and Public Health* 17, no. 8 (2024): 102486, https://doi.org/10.1016/j.jiph.2024.102486.

45. H. Krumbein, L. S. Kümmel, P. C. Fragkou, et al., "Respiratory Viral Co-Infections in Patients With COVID-19 and Associated Outcomes: A Systematic Review and Meta-Analysis," *Reviews in Medical Virology* 33, no. 1 (2023): e2365, https://doi.org/10.1002/rmv.2365.

46. M. J. Peluso, T. M. Deveau, S. E. Munter, et al., "Chronic Viral Coinfections Differentially Affect the Likelihood of Developing Long COVID," *Journal of Clinical Investigation* 133, no. 3 (2023): e163669, https://doi.org/10.1172/JCI163669.

## Supporting Information

Additional supporting information can be found online in the Supporting Information section.